Journal of Nuclear Materials 543 (2021) 152594

Contents lists available at ScienceDirect

Journal of Nuclear Materials

journal homepage: www.elsevier.com/locate/jnucmat

Thermal diffusivity of irradiated tungsten and tungsten-rhenium alloys

Masafumi Akiyoshi[a,*], Lauren M. Garrison[b], Josina W. Geringer[b], Hsin Wang[b], Akira Hasegawa[c], Shuhei Nogami[c], Yutai Katoh[b]

[a] Osaka Prefecture University, Sakai, Osaka 599-8570, Japan
[b] Oak Ridge National Laboratory, Oak Ridge, TN 37831, USA
[c] Tohoku University, Sendai, Miyagi 980-8579, Japan

ARTICLE INFO

Article history:
Received 4 March 2020
Revised 16 September 2020
Accepted 8 October 2020
Available online 15 October 2020

Keyword:
Thermal diffusivity
Tungsten material
Neutron irradiation
Transmutation
Lattice defect

ABSTRACT

The Japan-US PHENIX project irradiated tungsten materials in the RB-19J capsule experiment in the High Flux Isotope Reactor (HFIR). A gadolinium (Gd) shielding was used to absorb the thermal neutrons and reduce rhenium and osmium generation in tungsten. Pure tungsten and K-doped W-3% Re samples were irradiated at 532 – 662 °C to dose of 0.21-0.46 dpa, with the grain orientation perpendicular or parallel to the disk surface. Thermal diffusivity measurements were performed from 100 °C to 500 °C. Additional measurements followed after annealing up to 900 °C. Irradiated pure tungsten specimens showed similar thermal diffusivity results compared with an unirradiated W-1% Re specimen in another study. The transmutation amount of Re was calculated to be about 0.52% for those specimens that showed good agreement with this study. Specimens irradiated in this study to different doses presented almost the same thermal diffusivity. Annealing up to 800 °C resulted in no recovery of thermal diffusivity. These results show that the contribution of crystalline defects to degradation of thermal diffusivity is quite limited. In addition, the thermal diffusivity of the irradiated specimens was getting close to that of the unirradiated specimens at elevated temperature.

1. Introduction

Neutron irradiation introduces various changes in the physical properties of materials. Thermal diffusivity is an important property to consider as it is key in the divertor design for a fusion reactor. High heat transfer ceramic materials such as SiC or AlN showed severe degradation in thermal diffusivity after neutron irradiations [1-3]. In these materials, heat is mainly carried by phonon, and the heat transfer is disturbed by neutron induced defect with phonon-lattice scattering.

Tungsten is the primary candidate material for divertor in which some part of heat is carried by phonons like ceramics, and the other part is carried by electron like other metals. In fusion reactors neutron irradiation will induce both crystalline displacement defects and transmutation reactions producing rhenium and osmium. It was reported that the thermal diffusivity of tungsten is strongly reduced by additional elements in the alloy [4]. It is important to understand these effects independently for developing tungsten materials for fusion reactors. Currently, there is limited available data of tungsten on thermal diffusivity after neutron irradiation [5]. Furthermore, the existing irradiations were performed in fission test reactor with different neutron energy spectra from a fusion reactor. In a fission reactor, the ratio of thermal neutrons that induce transmutations to fast neutrons that induces crystalline defects is relatively higher than that in a fusion reactor. In the case of tungsten materials, the total solid transmutation rate in a fusion divertor is 0.08 %/dpa, while it is about 8.5 %/dpa in the fuel trap region of the HFIR at Oak Ridge National Laboratory (ORNL) [6]. Moreover, it has been reported that specimens irradiated in light-water fission reactors had different microstructures from materials irradiated in fast reactors [7].

Therefore, the US-Japan collaboration project PHENIX irradiated tungsten materials in the RB-19J capsule experiment in the HFIR. The capsule was lined with a 1 mm thick gadolinium (Gd) metal liner. It was located on the inside of the capsule housing and surrounded the specimen holders. Its purpose was to serve as a thermal neutron shield to modify the fast/thermal neutron ratio over the life of the experiment and controlling the rhenium (Re) and osmium (Os) transmutations [8,9].

* Corresponding author.
E-mail address: akiyoshi@riast.osakafu-u.ac.jp (M. Akiyoshi).

https://doi.org/10.1016/j.jnucmat.2020.152594
0022-3115/

Table 1
Neutron capture reactions in tungsten and rhenium material. Cross sections in this table are for thermal neutrons [13].

target nuclide	natural abundance (%)	cross section (barn)	produced nuclide	half life time of the produced nuclide	daughter nuclide
^{184}W	30.4	1.7	^{185}W	75.1day	^{185}Re
^{186}W	28.4	38	^{187}W	23.7h	^{187}Re
^{185}Re	37.4	112	^{186}Re	3.7day	^{186}Os
^{187}Re	62.6	76	^{188}Re	17h	^{188}Os

2. Experimental

For the PHENIX project, the HFIR neutron irradiation experiment in the RB-19J capsule was designed with three different temperature zones, each containing subholders, that was irradiated at about 550°C, 850°C and 1050°C to doses of 0.2 to 0.7 displacements per atom (dpa) during 4 HFIR irradiation cycle (cycle 466 to cycle 469) from June 14 to December 9, 2016. The total operation time was 94 days at a nominal power of 85 MW. The large irradiation capsule, RB-19J, was inserted in the Removable Beryllium (RB*) position of the HFIR. The RB* region is part of the reflector which is the concentric ring surrounding the control plates and outer fuel element of the HFIR. With typical experimental data, neutron flux at the flux trap region (used for rapid irradiation) is 1.1×10^{19} n/m^{2}s (E>0.1 MeV) and 1.7×10^{19} n/m^{2}s (<0.5 eV) while in the RB* region it is 4.7×10^{18} n/m^{2}s (E>0.1 MeV) and 9.5×10^{18} n/m^{2}s (E< 0.5 eV) at 85 MW operation [10]. As mentioned, the 1mm thick Gd shield surrounded the sub-holders in RB-19J, and it reduced the thermal neutrons from 1×10^{19} n/m^{2}s to an order of 1×10^{17} n/m^{2}s [11,12]. This reduction is because of the large capture cross section for thermal neutrons, ^{157}Gd (natural abundance 15.7 %): 2.5×10^5 barn and ^{155}Gd (natural abundance 14.8%): 6.1×10^4 barn (neutron capture cross section in this study is for 0.0253 eV thermal neutron from JENDL-4.0). In the capsule, more than 20 varieties of pure tungsten and tungsten alloys were irradiated.

After the irradiation, the tungsten specimens transmuted to the radio-nuclides as shown in Table 1.

In this study, thermal diffusivity measurements were performed on pure tungsten and K-doped W-3% Re disk samples that were 6 mm in diameter and 2 mm thick. The samples were made from stress relieved thick plate (produced by A.L.M.T.) with the grain orientation perpendicular or parallel to the disk surface [4,14]. The reduction ratios of these materials at rolling were 80% and the final heat-treatment temperature before the irradiation was 900°C for 20 min. Samples were cut from the original thick block so that the grain orientation is either elongated parallel or perpendicular to the sample surface.

These specimens were irradiated at 532-662 °C in same subcapsule of 550 °C zone to 0.21-0.46 dpa where the conversion from fluence to displacement per atom is obtained by dpa = 0.195 Φ_{fast} / 10^{25} n/m^2 (Φ_{fast} is fast neutron fluence (E>0.1 MeV)) for tungsten in HFIR [15]. The actual temperatures during irradiation were derived and calculated from a combination of data sources that included the data from thermocouples (used to control the temperatures inside the capsule during irradiation), passive SiC temperature monitors (specimens included inside the sub-holders to validate the temperatures at specific locations) that were measured post irradiation, and the thermal model used for the design of the capsule. The neutron fluence for each specimen was calculated from a model that was produced after post irradiation evaluation of the neutron fluence monitors. Due to HFIR's axial neutron flux profile, the fluence values for the specimens, in different sub-holders, largely depends on the axial position within the capsule. Due to the loss of one dosimeter during disassembly, only two dosimeters were available to estimate the neutron flux for RB-19J capsule. From the experimental data of the two samples, a parabolic function as $F = a(1+bz^2)$, where z is specimen axial position (cm) and a, b are constant derived from the data ($a = 1.02 \times 10^{20}$, $b=-1.86 \times 10^{-3}$ for thermal neutrons, E < 0.5 eV, and $a = 3.59 \times 10^{20}$, $b= -1.44 \times 10^{-3}$ for fast neutrons, E > 0.1 MeV) [12], is applied to estimate fast and thermal neutron flux for each specimen position. The dosimeters were positioned at an axial height of 2.7 cm and 15.2 cm above the HFIR core centerline while the 550°C zone specimens were positioned between the axial heights of 17 cm to 25 cm from the core centerline. Due to only two data points available, the thermal fluence model does not provide a good representation of the thermal fluence values, as some positions above ~23 cm height from the core centerline, gives negative values. The estimated fluence of thermal neutrons was 1.0×10^{24} n/m^2 and 5.8×10^{23} n/m^2 for each dosimeter. The details for each specimen are shown in Table 2.

The capsule was disassembled in the hot-cell facility and shipped to the Low Activation Materials Development and Analysis Laboratory (LAMDA) at ORNL in early 2018 after a cooling period.

Thermal diffusivity measurements were performed with a NETZSCH LFA-457 conventional thermal analyzer from 20 to 500 °C in an atmosphere of ultra high purity Ar gas flow. Additional measurements were done after annealing up to 900 °C. The annealing measurements were performed using a NETZSCH LFA-467HT hyper flash analyzer in atmosphere of vacuum with turbopump to 10^{-2} Pa to avoid oxidation of tungsten materials. Tungsten material is very sensitive to oxidation. After it was measured in LFA-457 at 500 °C, the surface of all specimens was slightly oxidized. The oxidation from activated tungsten easily vaporizes and that cause spread contamination, as well as the oxidation potentially influencing the thermal diffusivity measurements so it should be avoided. The surfaces of the specimens were coated with conventional graphite spray. In the case of thin specimen (0.5 mm thick for pure tungsten), the graphite layer affects the estimate of thermal diffusivity as mentioned below.

After the measurements up to 500 °C were performed for all four specimens, annealing experiments were performed on 5001 (pure tungsten) and A000 (K-doped W-3% Re). The grain orientation of both specimens is perpendicular to the disk surface. Usually, an isochronal annealing effect is measured after an annealing at an aimed temperature in another furnace and then the sample would be transferred to the thermal diffusivity measurement instrument. If that method is followed, heating and cooling time is required for annealing, and then after that, to obtain temperature dependence of thermal diffusivity for the specific specimen, additional heating and cooling is required. It requires about twice the time and increases the contamination risk and cost working with radioactive materials. For this reason, annealing measurements were performed in the furnace of LFA-467HT instead. For example, after the thermal diffusivity measurement up to 500 °C, the next measurements were performed from 100 °C to 600 °C at every 100 °C increments. At this aimed annealing temperature, 30 flash shots in the LFA-467HT were performed for 2 specimens (which takes more than 1 hour to complete). The next measurements were performed from 100 °C to 700 °C (again at 100 °C increments) to evaluate the annealing effect at 600 °C and to achieve the annealing at 700 °C, and so on.

Table 2
Detail of unirradiated and neutron irradiated specimens in Fig. 4.

Specimen ID	Irradiation temperature (°C)	Fast neutron fluence (10^{25} n/m^{2}s) E > 0.1MeV		Dose (dpa)		Component	Grain Orientation	Thermal diffusivity at RT (mm^2/s)	Degradation of thermal diffusivity (%)
		Calc.	Exp.	Calc.	Exp.				
4003	unirradiated					Pure W	∥	70.8	18.1
4000	662	2.4	2	0.46	0.39			58.0	
500H	unirradiated						⊥	73.8	20.7
5001	548	1.3	0.78	0.25	0.15			58.5	
9003	unirradiated					K-doped	∥	41.4	12.0
9000	532	1.1	0.53	0.21	0.1	W-3% Re		36.4	
A00C	unirradiated						⊥	41.9	8.3
A000	660	2.3	2	0.45	0.38			38.4	

3. Surface treatment

To measure thermal diffusivity with a flash method (on tungsten or any other polished metal specimens), a carbon coating is required. This improves absorbance of the flashed light on the front side and also infrared emission from the back side as described in the previous paper [17]. A conventional graphite spray such as 'GRAPHIT33' is used for thick standard specimens, but it results in relatively thick (> 10 μm) carbon layers on the surface of the specimen. It adds a non-negligible amount of additional time to thermal diffusion through thin specimen of high thermal diffusivity. To avoid this factor, NETZSCH Japan provides Graphene spray that gives only 1/20 weight of the layer compared with GRAPHIT33. This spray is provided as ' JA007159: Black coating agent for LFA on very thin specimen'. Fig. 1 shows the obvious difference between a D10TH specimen that was covered with graphite spray and the other specimens. It was measured using the NETZSCH-467HT with a pulse width fast enough to measure unirradiated pure tungsten with a 0.3 mm thickness. Here, the size of the disk specimen is described as DxTy, where Dx is the diameter of x mm and Ty is the thickness of y mm (for D10TH, the diameter is 10 mm and the thickness is 0.5 mm). The D6T2 (a 2 mm thick specimen) and D10T1 and D6T1 (both 1 mm thick specimens), were covered with graphite spray. These were all thick enough to ignore the additional diffusion time. The measurement of the D10TH (a 0.5 mm thick specimen), was repeated with a very thin coating of graphite spray and showed almost the same result as the other specimens. Therefore, to measure a 0.5 mm thick specimen using graphite spray requires careful treatment and it

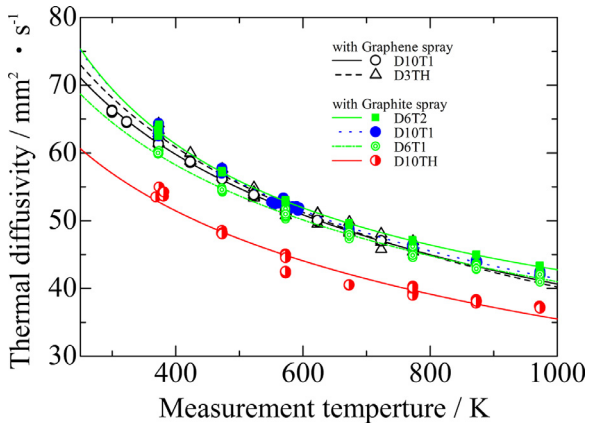

Fig. 1. Difference between graphene and graphite coatings on different size of polished pure tungsten specimens measured with a NETZSCH LFA-467HT. Disk specimen size is shown as DxTy, where Dx is the diameter of x mm and Ty is the thickness of y mm (for D10TH, the diameter is 10 mm and the thickness is 0.5 mm).

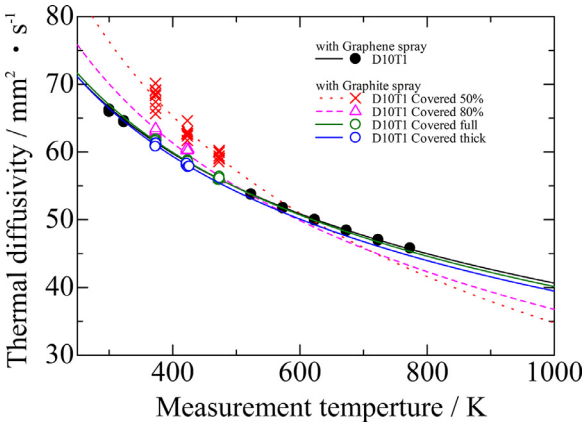

Fig. 2. The effect from density of the graphite coating on diameter of 10mm and thickness 1mm polished pure tungsten specimens measured with a NETZSCH LFA-467HT.

depends on the skill of the technician. The result of a slightly thick coating gives a large difference from the true value. It is therefore concluded that the graphene spray is necessary for reliable measurement with -TH specimen (0.5 mm thick).

Moreover, the effect from density of the graphite coating was validated in Fig. 2 using polished D10T1 pure tungsten specimens. A coating that is too thick, results in thermal diffusivity degradations, as described above. If the coating is too thin, the un-covered shiny surface gives large dispersion of thermal diffusivity. Fig. 3-A to D shows picture of different density of coating with conventional graphite spray in Fig. 2. As a result, for the measurement of D6T2 irradiated specimens, a relatively thick graphite coating was used.

4. Result

Fig. 4 shows the thermal diffusivity of irradiated and unirradiated tungsten materials. The thermal diffusivity values at room temperature (300 K) were extrapolated by a fitting function to the data collected at higher temperature for each specimen, as shown in Table 2. The open and black symbols in Fig. 4 represent the unirradiated specimens and the filled and red symbols represent the irradiated specimens.

The irradiated pure tungsten specimens show thermal diffusivity values of 18.1% and 20.7% lower than those of unirradiated specimens at room temperature. The differences become smaller at higher temperatures. For the case of K-doped W-3% Re specimens, the degradations after irradiation are 12.0 % and 8.3% compared to unirradiated K-doped W-3% Re specimens, which shows a small dependence on the measurement temperature. With respect to grain orientation, there is almost no visible difference observed

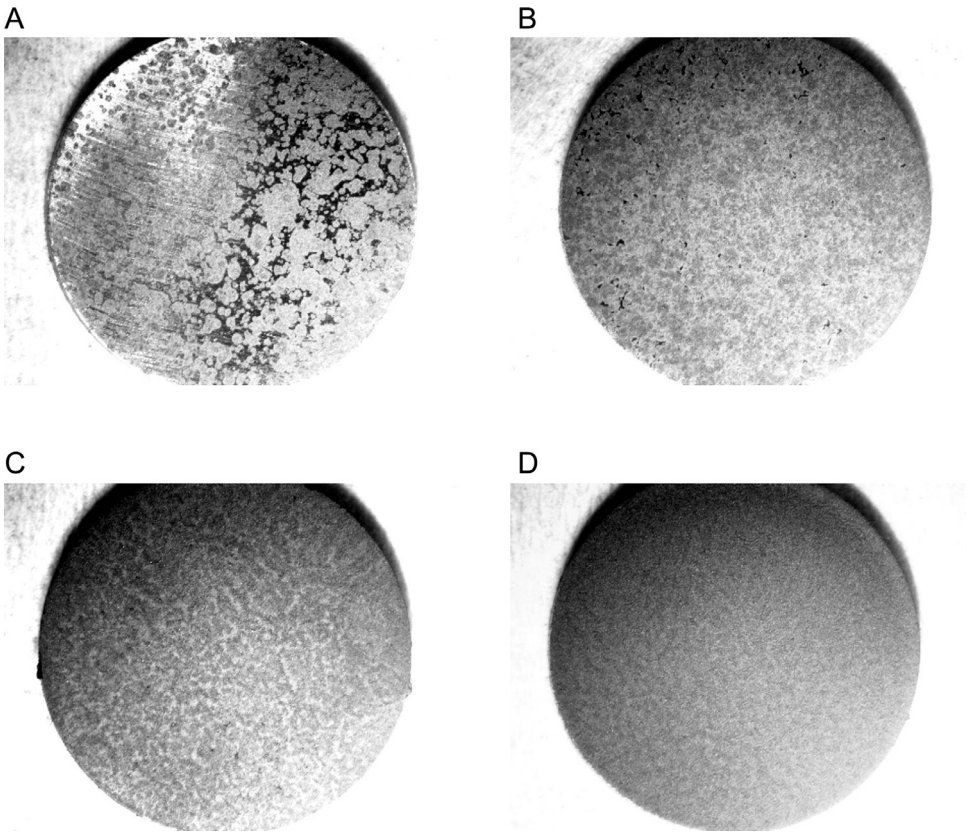

Fig. 3. Different density of graphite coatings on D10T1 polished pure tungsten specimens measured in Fig. 3. The cover ratio is a rough estimation for easy understanding.

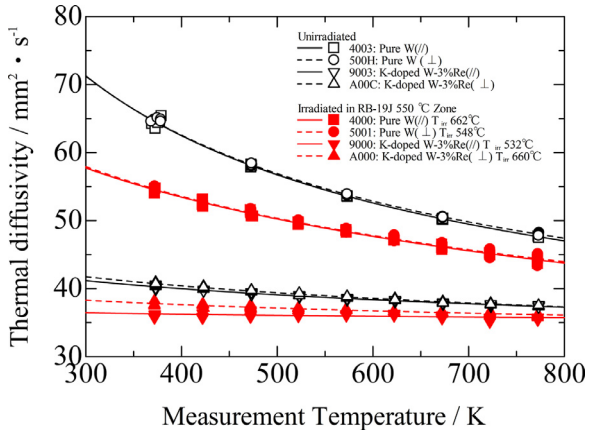

Fig. 4. Thermal diffusivity of the as-irradiated and the unirradiated tungsten materials. The open and black symbols represent unirradiated specimens and the filled and red symbols for irradiated specimens.

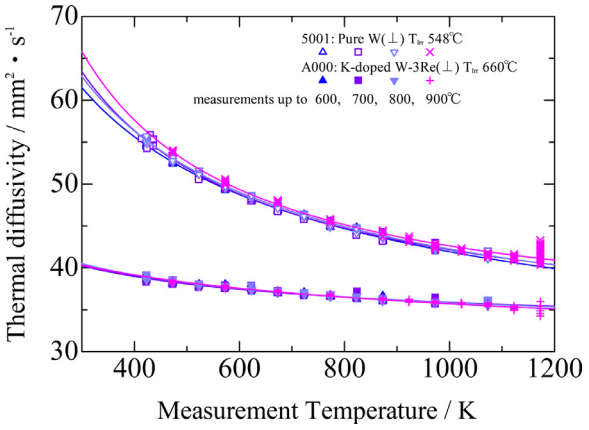

Fig. 5. Thermal diffusivity of the irradiated tungsten materials after annealing up to 900 °C. After an annealing at aimed temperature, dependence on temperature was estimated during increasing temperature to next aimed annealing temperature.

for pure tungsten demonstrated by the overlap of the two specimens, 4000 and 5001, while a small difference is shown for the irradiated K-doped W-3% Re. It is to be noted that all the specimens, even though irradiated in the same capsule, may have slightly different irradiation temperature and dose, which is dependent on the individual specimen position within the capsule. For instance for the K-doped W-3% Re material, the dose of A000 is 2.1 times larger than 9000.

After the as-irradiated measurement up to 500 °C, which is lower than the irradiation temperature of the specimens, the annealing measurements were performed. For the annealing measurements as described in the Experimental section, one sample each of the pure W and the K-doped W-3% Re were repeatedly cycled between high temperatures and room temperature, with the maximum temperature rising from 600 to 900°C in 100 degrees increments. The samples were held for approximately 1 hour at the maximum temperature during each annealing step. Fig. 5 shows the results. In this figure, the triangle symbols pointing upwards represent measurements up to a maximum of 600 °C. The results below 500 °C match the temperature dependence for the 'as-irradiated' tungsten, as in Fig. 4. The next step, the square symbols represent measurements after the previous 600 °C annealing treatment. In this step, measurements were performed up to a maximum of 700 °C. Fig. 5 demonstrates that both pure tungsten (5001) and K-doped W-3% Re (A000) specimens show no recovery in their

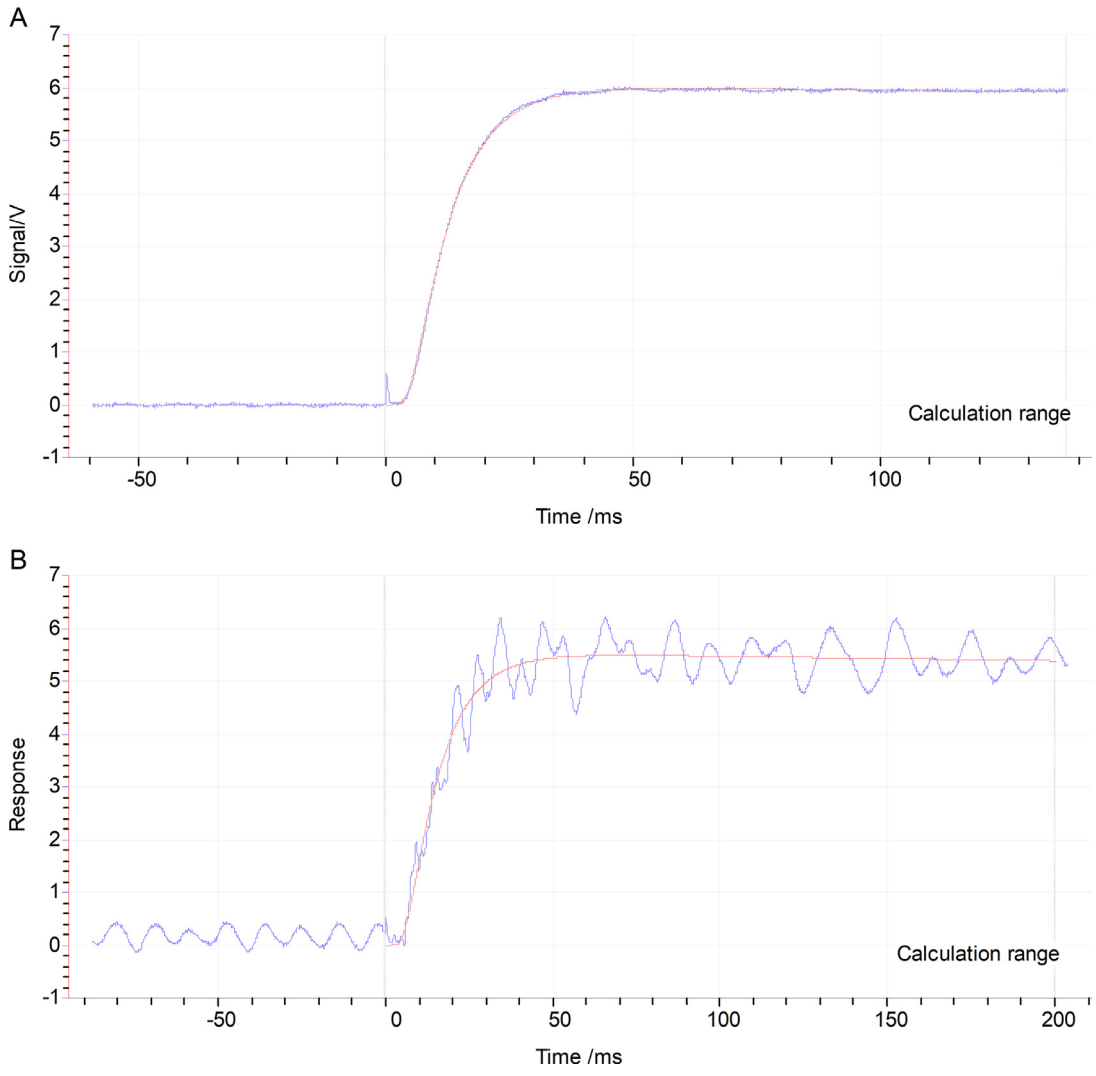

Fig. 6. Infrared signal from pure tungsten (irradiated:5001) with a measurement at 300 °C and at 900°C. At 900°C measurement, obvious oscillation was observed on the IR signal.

thermal diffusivity for annealed results up to 800 °C. The annealing measurement process stopped at 900 °C because the measurements performed at 900 °C showed severe oscillation on the infrared (IR) signals as displayed in Fig. 6. This IR signal is used to evaluate the temperature change of the back side of the specimen after exposure to the flash light. Usually, the intensity of an IR signal is increases based on the Planck's law, so the intensity ratio before and after a flash shot gets larger with the increasing measurement temperature, even if the absolute temperature change before and after a flash is the same. Nevertheless, several measurements are quite noisy, due to the IR signal with oscillation at a constant frequency (about 100 Hz). These noisy signals resulted in a large dispersion of the thermal diffusivity measurements. At this time, this problem is not clarified and because it was worse at higher temperatures, the measurements were stopped at 900°C.

5. Discussion

In Fig. 4, pure tungsten specimens show obvious degradation in thermal diffusivity after irradiation, however it is still higher than that of unirradiated K-doped W-3% Re specimens. Fukuda et al., reported tungsten-rhenium alloy showed a systematic change with rhenium concentration, but on the other hand, K-doped W showed almost same thermal diffusivity [4]. In their paper, W-1% Re alloy showed 47.6 mm^2/s at 401 °C, and this thermal diffusivity is very close to that of the irradiated pure tungsten in this study. If a pure tungsten specimen is irradiated in HFIR in the flux trap

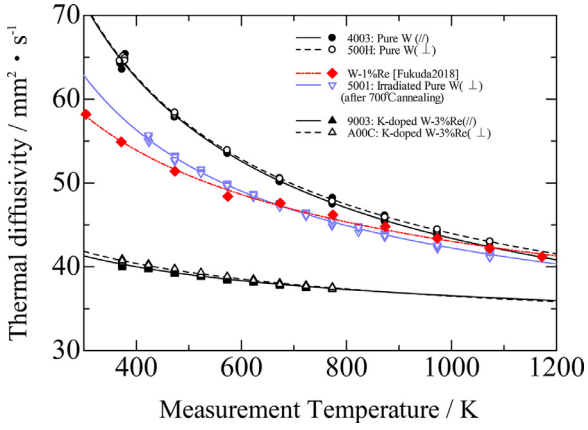

Fig. 7. Comparison of the thermal diffusivity between W-1% Re alloy [Fukuda2018] and the result in this study. The neutron irradiated pure tungsten showed similar result with the W-1% Re alloy.

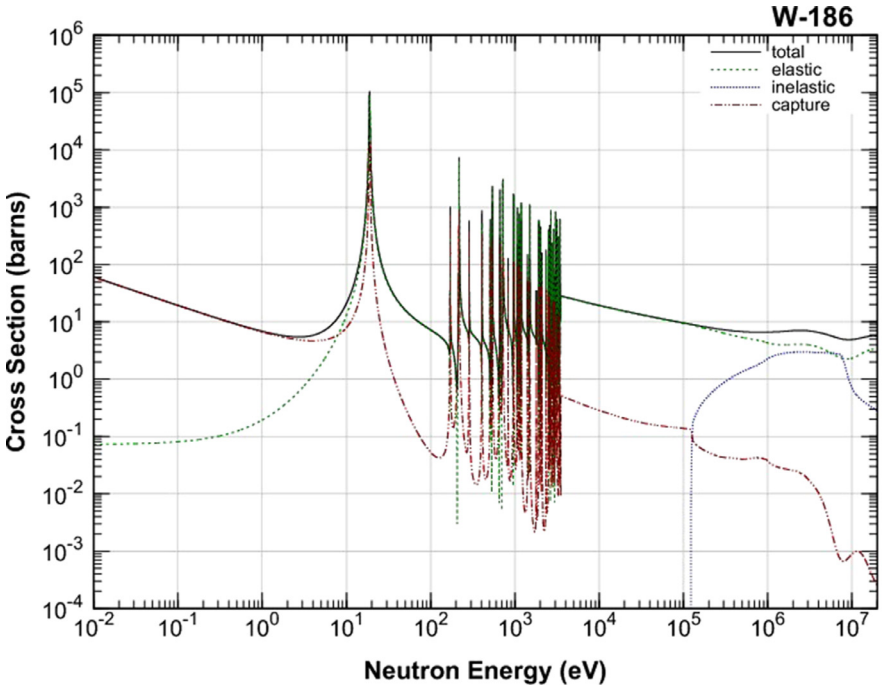

Fig. 8. Neutron reaction cross section for ^{186}W from JENDL-4.0 library.
(https://wwwndc.jaea.go.jp/j40fig/jpeg/w186_f1.jpg)

region without a gadolinium shield to the same dpa as in this study, transmuted rhenium reaches 1.8-3.9% [6]. It shows that the gadolinium shield in RB-19J capsule reduce transmutation successfully.

Thermal diffusivity of W-1% Re alloy showed good agreement with neutron irradiated pure tungsten in this study as in Fig. 7. Tungsten has a higher transmutation probability with lower energy neutrons, so the thermal neutron fluence is a key factor for the amount of transmutation the material accumulates in a reactor. For a rough estimation of transmutation, 5×10^{23} n/m^2 is used as thermal neutron fluence $\Phi_{thermal}$. From the Table 2, the cross-section σ of neutron capture reaction ^{186}W(n,γ)^{187}W is 38.1 barn (10^{-28} m^2), and the natural abundance θ of ^{186}W is 28.4%. The ^{187}W is a radioactive isotope of tungsten and beta-decays to ^{187}Re. Therefore, the transmutation ratio for this isotope at the assumed thermal neutron fluence is obtained as $\Phi_{thermal}\ \sigma\ \theta = 5.4 \times 10^{-4}$. The reaction ^{184}W (n,γ)^{185}W and beta-decay create ^{185}Re, where $\sigma = 1.7$ and $\theta = 30.6$ % that result in 2.6×10^{-5}. This rough estimation gives transmuted ^{187}Re ratio by thermal neutron, about 0.06%. Although the cross sections for transmutation in tungsten are higher for lower energy neutrons, there is a noticeable contribution from higher energy neutrons as well. Taking the full HFIR neutron energy spectrum into account and including the effect on the spectrum of the thermal neutron shield, Charles R. Daily from ORNL reported a transmutation ratio of 0.52% for 550°C zone in 2016. ^{186}W shows large resonance absorption around 20eV as shown in Fig. 8 [16]. Also, epithermal neutrons (0.5eV to 110keV) estimated by the neutron dosimeters in the capsule showed 50 times higher flux than the thermal neutron flux. Thus, using the full neutron spectrum calculation gives a higher transmutation than our estimation using only the thermal neutron reactions for two isotopes. The transmutation ratio of 0.52% is in good agreement with the results in this study. The calculation still has some error that comes from the dose estimation precision. Experimental elemental analysis of some of the irradiated samples is required for comparison with the calculation. Furthermore, the distribution of transmuted rhenium in irradiated specimens must be investigated.

Finally, fast neutrons induce crystalline defects that affect phonon transfer. In the Table 1, the fast neutron fluence (E>1MeV) is listed for each specimen where 'Exp.' represent the result from two dosimeters and 'Calc.' represent the simulation result based on the known neutron flux of HFIR and scatter/capture reactions. There is a factor of 2 to 4 difference between 4001 and 5001 (pure tungsten) and between 9000 and A000 (K-doped W-3% Re). In these pairs of the same material samples, orientation of grain is different, that is parallel or perpendicular to the sample surface. Though in the case of the unirradiated specimen, the thermal diffusivity perpendicular to the disk plane is almost same no matter the grain orientation. Furthermore, the irradiated specimens of these pairs show almost the same results in spite of the large dose difference. In addition, the irradiation temperature is also different and the lower dose specimens were irradiated at lower temperature. It is not entirely expected that these samples irradiated at different doses and temperatures would have such similar thermal diffusivities. One possible explanation is that because the samples irradiated to higher dose were also the ones irradiated at higher temperature, this combination may have caused more self-healing during irradiation and resulted in fewer remaining defects after irradiation than if they had been irradiated at a lower temperature. The distribution of crystalline defects in these specimens and the recovery with annealing can be estimated in the future with positron annihilation lifetime spectroscopy (PALS).

For more detail, many specimens irradiated at different conditions in RB-19J capsule must be compared. Most specimens intended for thermal diffusivity measurement are of a D3TH type, which are 3mm diameter and 0.5mm thick small disks. For these small specimens, the oscillation of the IR signal at high temperature is more significant than in Fig. 6, and that leads to a large dispersion in thermal diffusivity. Further study on surface treatment and measurement conditions, especially the flash pulse width, must be done to resolve this problem. Furthermore, another irradiation experiment without gadolinium shielding in HFIR rabbit capsules has been performed. In this capsule, several tungsten and

tungsten alloy materials were irradiated to lower dose but higher transmutation. It will give a good comparison with the result in this study.

6. Conclusion

Tungsten materials were irradiated in the ORNL HFIR with gadolinium shielding to absorb thermal neutrons and reduce rhenium generation in the tungsten. Pure tungsten and K-doped W-3% Re samples were irradiated at 532 – 662 °C to 0.21-0.46 dpa, with the grain orientation perpendicular or parallel to the disk surface. Irradiated pure tungsten specimens shows 18.1% and 20.7% (depending on the grain orientation) lower thermal diffusivity than that of unirradiated specimens, and K-doped W-3% Re specimens showed 12.0% and 8.3% degradation for the two grain orientations of that material. Specimens with different orientation showed almost the same thermal diffusivity before and even after the irradiation at different doses. The irradiated pure tungsten showed higher thermal diffusivity than the unirradiated K-doped W-3% Re material. It shows that the amount of transmutation was limited by the gadolinium shield successfully. W-1% Re specimen in another study showed similar result to this irradiated pure tungsten. The transmuted amount of rhenium was calculated to be about 0.52% for these specimens, and that shows good agreement with this study. Further more, annealing beyond the irradiation temperature, up to 800 °C resulted in no recovery of thermal diffusivity. These results support the hypothesis that crystalline defects like vacancies in tungsten has a quite limited effect on thermal diffusivity. Therefore, transmutation calculation gives a reasonable forecast of thermal diffusivity after an irradiation.

Data Availability

The raw data required to reproduce these findings are available to download from http://bigbird.riast.osakafu-u.ac.jp/~akiyoshi/DataAvailability/20200304_ICFRM-19.LZH that contains NETZSCH mdb data for Proteus 7 and smp graph data created by SMA4Win.

Declaration of Competing interest

The authors declare that they have no known competing financial interests or personal relationships that could have appeared to influence the work reported in this paper.

CRediT authorship contribution statement

Masafumi Akiyoshi: Conceptualization, Investigation, Writing - original draft. **Lauren M. Garrison:** Investigation, Writing - review & editing. **Josina W. Geringer:** Investigation, Writing - review & editing. **Hsin Wang:** Investigation. **Akira Hasegawa:** Resources. **Shuhei Nogami:** Resources. **Yutai Katoh:** Project administration.

Acknowledgement

This work was performed as part of the U.S.-Japan PHENIX Cooperation Collaboration Project on Technological Assessment of Plasma Facing Components for DEMO Reactors, supported by the U.S. Department of Energy, Office of Science, Fusion Energy Sciences and Ministry of Education, Culture, Sports, Science and Technology, Japan. ORNL research sponsored by the U.S. Department of Energy, Office of Fusion Energy Sciences, under contract DE-AC05-00OR22725 with UT-Battelle, LLC.

Supplementary materials

Supplementary material associated with this article can be found, in the online version, at doi:10.1016/j.jnucmat.2020.152594.

References

[1] M. Akiyoshi, T. Yano, Y. Tachi, H. Nakano, Saturation in degradation of thermal diffusivity of neutron-irradiated ceramics at 3×10^{26}n/m^2, J. Nucl. Mater. 367-370 (2007) 1023–1027.
[2] M. Akiyoshi, T. Yano, Neutron-irradiation effect in ceramics evaluated from macroscopic property changes in as-irradiated and annealed specimens, Prog. Nucl. Energy 50 (2008) 567–574.
[3] M. Akiyoshi, Thermal diffusivity of ceramics at the neutron irradiation temperature estimated from post-irradiation measurements at 123-413 K, J. Nucl. Mater. 386-388 (2009) 303–306.
[4] M. Fukuda, A. Hasegawa, S. Nogami, Thermal properties of pure tungsten and its alloys for fusion applications, Fusion Eng. Des 132 (2018) 1–6.
[5] M. Fujitsuka, B. Tsuchiya, I. Mutoh, T. Tanabe, T. Shikama, Effect of neutron irradiation on thermal diffusivity of tungsten-rhenium alloys, J. Nucl. Mater. 283-287 (2000) 1148–1151.
[6] M.E. Sawan, Transmutation of Tungsten in Fusion and Fission Nuclear Environments, Fusion Sci. Tech 66 (2014) 272–277.
[7] A. Hasegawa, M. Fukuda, K. Yabuuchi, S. Nogami, Neutron irradiation effects on the microstructural development of tungsten and tungsten alloys, J. Nucl. Mater. 471 (2016) 175–183.
[8] L.M. Garrison, Y. Katoh, J.W. Geringer, M. Akiyoshi, PHENIX U.S.-Japan Collaboration Investigation of Thermal and Mechanical Properties of Thermal Neutron-Shielded Irradiated Tungsten, Fusion Sci. Technol 75 (2019) 1–11.
[9] Y. Katoh, D. Clark, Y. Ueda, Y. Hatano, et al., Progress in the U.S./Japan PHENIX Project for the Technological Assessment of Plasma Facing Components for DEMO Reactors, Fusion Sci. Technol 72 (2017) 222–232.
[10] T. Daly, J.L. McDuffee, Experimental and computational study of the flux spectrum in materials irradiation facilities of the High Flux Isotope Reactor, Proc. of 2012 Advances in Reactor Physics Linking Research, Industry, and Education (PHYSOR 2012).
[11] J.L. McDuffee, C.R. Daily, N.O. Cetiner, C.M. Petrie, J.W Geringer, HFIR-MFE-RB-19J Thermal and Neutronic Design, Fusion Mater. Semiannual Prog. Rep (2016) 205 DOE/ER-0313/60.
[12] L.R. Greenwood, B.D. Pierson, T. Trang-Le, HFIR-MFE-RB-19J neutron fluence measurements and radiation damage calculations (REVISED), Fusion Mater. Semiannual Prog. Rep (2019) 160 DOE/ER-0313/67.
[13] Isotope handbook 11th edition, Japan radioisotope association, 2011 Maruzen, Japan.
[14] S. Nogami, W. Guan, A. Hasegawa, M. Fukuda, Feasibility of Utilizing Tungsten Rod for Fusion Reactor Divertor, Fusion Sci. Technol 72 (2017) 673–679.
[15] M. E.Sawan, Damage parameters of structural materials in fusion environment compared to fission reactor irradiation, Fusion Eng. Des 87 (2012) 551–555.
[16] K. Shibata, et al., JENDL-4.0: A New Library for Nuclear Science and Engineering, J. Nucl. Sci. Technol. 48 (2011) 1–30.
[17] M. Akiyoshi, R. Kasada, Y. Ishibashi, L.M. Garrison, J.W. Geringer, W.D. Porter, Y. Katoh, Validation of miniature test specimens for post-irradiation thermal diffusivity measurement, Fusion Eng. Des 136 Part A (2018) 513–517.